Environ Earth Sci (2010) 60:633–642
DOI 10.1007/s12665-009-0203-5

ORIGINAL ARTICLE

Hydrogeochemical genesis of groundwaters with abnormal fluoride concentrations from Zhongxiang City, Hubei Province, central China

Qinghai Guo · Yanxin Wang · Qingshan Guo

Received: 25 December 2008 / Accepted: 27 May 2009 / Published online: 11 June 2009

Abstract The groundwaters from Zhongxiang City, Hubei Province of central China, have high fluoride concentration up to 3.67 mg/L, and cases of dental fluorosis have been found in this region. To delineate the nature and extent of high fluoride groundwaters and to assess the major geochemical factors controlling the fluoride enrichment in groundwater, 14 groundwater samples and 5 Quaternary sediment samples were collected and their chemistry were determined in this study. Some water samples from fissured hard rock aquifers and Quaternary aquifers have high fluoride concentrations, whereas all karst water samples contain fluoride less than 1.5 mg/L due to their high Ca/Na ratios. For the high fluoride groundwaters in the fissured hard rocks, high HCO_3^- concentration and alkaline condition favor dissolution of fluorite and anion exchange between OH^- in groundwater and exchangeable F^- in some fluoride-bearing minerals. For fluoride enrichment in groundwaters of Quaternary aquifers, high contents of fluoride in the aquifer sediments and evapotranspiration are important controls.

Keywords Fluoride · Groundwater · Hydrogeochemistry · Anion exchange · Evaporation · Zhongxiang City

Q. Guo (✉) · Y. Wang
MOE Key Laboratory of Biogeology and Environmental Geology, School of Environmental Studies, China University of Geosciences, Wuhan, Hubei 430074, People's Republic of China
e-mail: qhguo2006@gmail.com; qhguo@tom.com

Q. Guo
Affiliated Hospital of Jingmen University, 448000 Jingmen, Hubei, People's Republic of China

Introduction

Fluorosis is an endemic disease due to long-term intake of excessive fluoride. So far two main kinds of fluorosis, namely dental fluorosis and skeletal fluorosis, have been identified. Patients with dental fluorosis chronically develop yellowing of teeth and pitting or mottling of enamel (Rwenyonyi et al. 2000; Vieira et al. 2005). Skeletal fluorosis is a bone disease exclusively caused by consumption of about ten times of the normal amount of fluoride (Krishnamachari 1986). Mild cases of skeletal fluorosis cause slight symptoms or problems. However, in serious cases, skeletal fluorosis results in unbearable pain as well as severe damage to bones and joints. In addition, fluorosis can also be manifested in central nervous system, visual organ or some soft tissues, such as muscles and ligaments (Cao 1990).

Although fluorosis can be triggered by anthropogenic enrichment of fluoride, endemic fluorosis resulting from exposure to geogenic fluoride is more frequent in distribution. There are several commonly accepted causes for endemic fluorosis: (1) long-term intake of high fluoride groundwater (Rukah and Alsokhny 2004), (2) exposure to high fluoride gas from coal burning (Wang and Huang 1995) or intake of high level fluoride from coal combustion-contaminated grains (Liang 1993), and (3) drinking brick tea in excess. With respect to brick tea-type fluorosis, western China (especially Tibet), where brick tea has been widely produced and consumed, is the major impacted area (Cao et al. 1997, 2000). Compared to food and brick tea, groundwater used for drinking is a more important source for human intake of fluoride. Common natural fluoride sources in groundwater are the dissolution of some fluoride bearing minerals, such as fluorite, amphiboles (e.g., hornblende, tremolite), fluorapatite and some micas weathered from

silicates, igneous and sedimentary rocks, especially shale (Datta et al. 1996). Unstable minerals such as sepiolite and palygorskite may also have a dominant control on fluoride concentration in groundwater (Jacks et al. 2005). In view of the hazard of drinking high fluoride groundwater, the World Health Organization (WHO) set the upper limits of F concentration in drinking water as 1.5 mg/L (WHO 1984).

In the world, there are many countries and districts where endemic fluorosis has been reported, including India (Gupta et al. 1999; Saxena and Ahmed 2003; Rao and Devadas 2003; Jacks et al. 2005), Kenya (Gaciri and Davies 1993; Moturi et al. 2002), Mexico (Grimaldo et al. 1995), Ghana (Apambire et al. 1997), Tanzania (Nanyaro et al. 1984), Ethiopia (Gizaw 1996), and Estonia (Karro et al. 2006). China is among countries most seriously affected by endemic fluorosis, with 40,210,000 patients of dental fluorosis and 1,730,000 of skeletal fluorosis (Luo and Yang 2000), mostly in north China, northwest China, and southwest China (Wang and Huang 1995; Dai et al. 2004). Endemic fluorosis has also been reported in Hubei Province of central China for this study (Wu et al. 1999; Luo and Yang 2000).

Zhongxiang City, located in central Hubei Province, is one of the eight waterborne fluorosis-impacted areas in Hubei, and groundwater has been the major source for water supply. Groundwaters with fluoride concentration up to 3.67 mg/L occur in some wells of the city. More importantly, dental fluorosis cases were identified in Huangpo village of the City during our field investigation. Therefore, delineating high fluoride groundwater zones and understanding basic hydrogeochemical processes controlling fluoride enrichment are extremely important for water resource management and human health at Zhongxiang.

The main objectives of this study are to: (1) characterize the hydrogeochemistry of the study area, (2) evaluate the extent of fluoride concentration in different types of groundwater, and (3) assess the main geochemical factors controlling fluoride enrichment.

General hydrogeology

Zhongxiang City is located in the central part of Hubei Province with an area of 4,488 km^2. The average annual air temperature in the recent 40 years at Zhongxiang is 15.9°C, with extreme high and low air temperature being 39.7 and −15.3°C, respectively. The average annual rainfall in the past four decades is 942.9 mm, and as much as 65% out of rainfall in a year is concentrated in the period from April to July. The average annual water surface evaporation is 1,444.0 mm.

Bedrocks outcropping in and around Zhongxiang City include the Upper Proterozoic dolomite rock, tillite, and siliceous rock, Cambrian and Ordovician dolomite rock, marl and carbonaceous shale, Silurian shale and siltstone, Permian–Triassic shale and sandstone, and Cretaceous–Lower Tertiary sandstone, siltstone, and mudstone (Fig. 1). Quaternary sediments with thickness from 50 to 150 m also occur at Zhongxiang, and the sediment types include mainly Holocene alluvium, proluvium and lacustrine deposit, Upper Pleistocene alluvium, Middle Pleistocene alluvium and proluvium, and Lower Pleistocene glacial deposit (Fig. 1). Moreover, the Jinningian granite outcrops only in the southwest (Fig. 1). The types of aquifers in the study area include carbonate aquifers, hard rock aquifers with groundwater in fissures, and Quaternary aquifers. The hostrocks of the karst aquifers consist mainly of the Upper Proterozoic and Lower Paleozoic dolomite rocks with very thin gypsum interlayers. The hard rock aquifers are composed of the Cretaceous and Tertiary sandstone with gypsum interlayers or the Jinningian biotite granite, and the Quaternary sediments of alluvium and proluvium constitute the Quaternary aquifers.

Groundwater in the study area is recharged by meteoric water, while the major ways of discharge include spring outflow, evaporation and artificial abstraction. Among the three types of aquifers, water storage decreases in the following sequence: the Quaternary aquifers, the karst aquifers, and the hard rock aquifers, with the greatest yield of 1,500, 1,000, and 10 m^3/day, respectively.

Sampling and analysis

Fourteen groundwater samples including four from fissured aquifers, three from karst aquifers, and seven from Quaternary porous aquifers, were collected in April 2008, and the locations of these samples are shown in Fig. 1. Among these samples, three have water temperatures more than 25°C, and the other 11 less than 25°C. Moreover, four and ten of these samples were collected, respectively, from springs and wells (Table 1).

When sampling, all water samples were filtered through 0.45 μm membranes on site. Samples were stored in new 300 mL polyethylene bottles that had been rinsed with deionized water twice before sampling. For metallic element analysis, reagent-quality HNO_3 with molar concentration up to 14 mol/L was added to one of these polyethylene bottles until the pH of the samples reached 1. Unstable hydrochemical parameters including water temperature, pH, and EC were measured in situ using portable temperature meter, pH meter, and electric conductivity meter that had been calibrated before use. Alkalinity was measured using the Gran titration method (Appelo and Postma, 1996). The concentrations of SO_4^{2-}, Cl^-, F^-, and NO_3^- were determined using ion chromatography (IC),

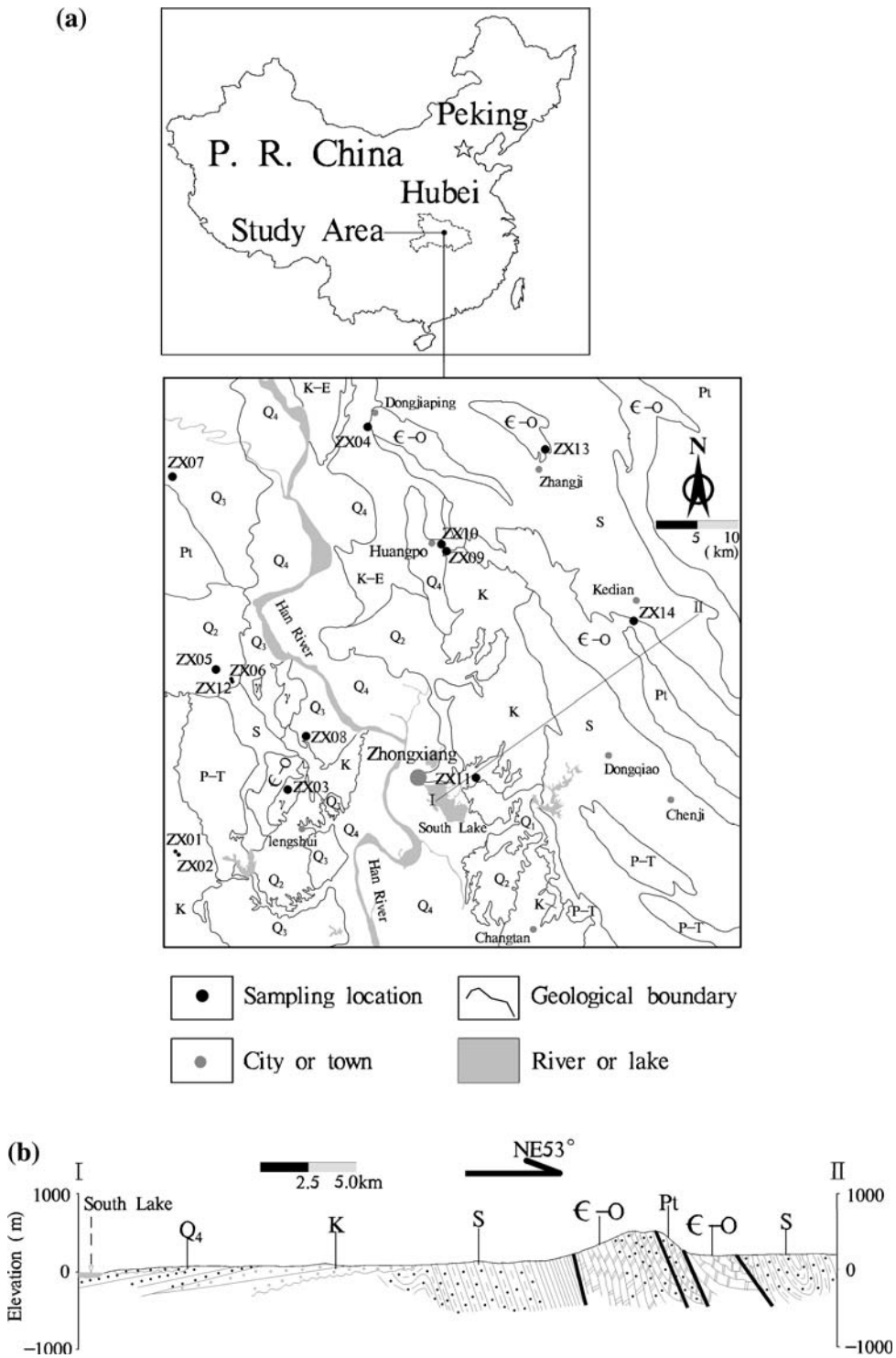

Fig. 1 **a** Simplified geological map of the study area and groundwater sampling locations and **b** geological cross section along the I–II line. *Pt* Upper Proterozoic dolomite rock, tillite, and siliceous rock; ∈–*O* Cambrian and Ordovician dolomite rock, marl and carbonaceous shale; *S* Silurian shale and siltstone; *P–T* Permian–Triassic shale and sandstone; *K–E* Cretaceous–Lower Tertiary sandstone, siltstone, and mudstone; Q_1 Lower Pleistocene glacial deposit; Q_2, Middle Pleistocene alluvium and proluvium; Q_3, Upper Pleistocene alluvium; Q_4, Holocene alluvium, proluvium and lacustrine deposit; γ Jinningian granite. Note that the locations of sediment samples RR01, RR02, RR03, RR04, and RR05 are the same to those of water samples ZX10, ZX09, ZX05, ZX08, and ZX11, respectively

SiO_2 using colorimetry, and other chemical constituents (Ca^{2+}, Mg^{2+}, Na^{+}, K^{+}, and Sr^{2+}) using inductively coupled plasma mass spectrometer (ICP-MS) within 2 weeks after sampling. The major properties (including water type, water temperature, sampling depth, etc.) and the hydrochemistry of all water samples are summarized in Tables 1 and 2, respectively.

Five Quaternary sediment samples were collected in this study as well, and their mineral compositions were determined using X-ray powder diffractometry (XRD) and given in Table 3. Moreover, the concentrations of total fluoride as well as fluoride in five different forms (namely water soluble fluoride, exchangeable fluoride, fluoride bound to Fe/Mn oxides, fluoride bound to organic matter

Table 1 Sampling site characteristics and some properties of water samples from Zhongxiang

No.	Longitude	Latitude	Sampling stratum	Burial depth	Water type	*T*	pH	EC
ZX01	112.28809	31.07964	Fissured hard rock aquifer	5	Cold well water	18.2	7.62	1375
ZX02	112.28885	31.07952	Fissured hard rock aquifer	2	Cold well water	17.0	7.24	783
ZX03	112.42884	31.14967	Fissured hard rock aquifer	–	Warm spring water	29.8	8.03	701
ZX04	112.53712	31.54688	Fissured hard rock aquifer	–	Warm spring water	48.2	7.96	922
ZX05	112.33926	31.28225	Quaternary aquifer	5	Cold well water	20.5	7.50	1385
ZX06	112.35877	31.27171	Quaternary aquifer	7	Cold well water	18.7	7.80	1482
ZX07	112.28646	31.49487	Quaternary aquifer	10	Cold well water	18.3	7.16	784
ZX08	112.45320	31.20810	Quaternary aquifer	6	Cold well water	17.5	7.35	1084
ZX09	112.63004	31.41617	Quaternary aquifer	2	Cold well water	17.2	7.94	1347
ZX10	112.62954	31.41674	Quaternary aquifer	–	Cold spring water	20.6	7.85	2063
ZX11	112.66907	31.15968	Quaternary aquifer	7	Cold well water	18.4	7.52	877
ZX12	112.35991	31.26862	Karst aquifer	110	Cold well water	21.4	7.80	713
ZX13	112.76418	31.51928	Karst aquifer	6	Cold well water	17.0	7.16	311
ZX14	112.87344	31.32888	Karst aquifer	–	Warm spring water	31.1	7.65	621

Burial depth in m, temperature in °C and EC in μS/cm

Table 2 Concentrations of major chemical constituents and TDS values of water samples from Zhongxiang

No.	HCO_3^-	SO_4^{2-}	Cl^-	F^-	NO_3^-	Ca^{2+}	Mg^{2+}	Na^+	K^+	Sr^{2+}	SiO_2	TDS
ZX01	237.5	142.0	81.0	0.64	12.0	96.0	14.2	86.0	1.3	0.42	19.5	571.7
ZX02	195.3	106.3	62.8	0.10	8.0	35.3	10.9	106.4	2.3	0.40	19.9	450.0
ZX03	288.3	8.2	3.6	3.25	–	8.6	5.8	84.5	3.1	1.19	20.9	283.2
ZX04	341.7	58.0	42.3	3.67	2.9	22.6	21.5	102.2	2.9	0.63	27.6	455.2
ZX05	291.9	168.0	63.6	0.32	158.0	136.7	36.8	32.9	5.8	0.63	15.9	764.6
ZX06	351.9	337.0	73.1	0.52	–	118.0	63.2	62.0	1.9	0.72	16.3	848.7
ZX07	281.0	19.0	51.1	0.05	19.2	83.4	14.1	31.2	3.2	0.40	13.4	375.5
ZX08	483.4	38.4	22.4	0.08	2.3	122.6	36.5	9.1	0.5	0.68	13.9	488.2
ZX09	494.3	95.6	124.0	1.88	99.3	90.2	51.6	140.3	3.3	0.50	17.7	871.5
ZX10	244.1	990.0	39.6	3.51	–	168.8	66.8	241.7	8.8	2.31	27.8	1671.3
ZX11	218.5	60.6	29.4	0.72	109.0	62.3	30.0	34.1	1.5	0.56	13.5	450.9
ZX12	421.0	21.1	5.1	0.30	3.2	74.8	40.1	6.0	0.5	0.14	9.8	371.5
ZX13	161.1	4.9	3.2	0.40	–	28.8	9.5	13.6	0.4	0.15	9.0	150.6
ZX14	328.3	44.2	2.6	1.15	2.0	70.5	30.0	1.7	0.8	0.33	7.1	324.6

The units are in mg/L. Note that the units of bicarbonate, sulfate and nitrate are mg HCO_3/L, mg SO_4/L, and mg NO_3/L, respectively

and residual fluoride) of two sediment samples (RR01 and RR02) collected from the Huangpo village with high fluoride groundwater in Quaternary aquifers were measured using ultraviolet spectrophotometer. During the sample preparation, total fluoride was extracted from sediment samples using 16.75 mol/L NaOH solution, and water soluble fluoride, exchangeable fluoride, fluoride bound to Fe/Mn oxides, and fluoride bound to organic matter were extracted with sequential chemical extraction procedure. The concentrations of fluoride in all kinds of forms are listed in Table 4.

Results and discussion

Groundwater chemistry

In general, the groundwater chemistry varies with different occurrence conditions. For the groundwaters from hard rock aquifers, the pH values are between 7.24 and 8.03, and the TDS values between 283.2 and 571.7 mg/L. For the karst groundwaters, the pH and TDS values are from 7.16 to 7.80 and from 150.6 to 371.5 mg/L, respectively. In contrast, the groundwaters occurring in Quaternary

Table 3 Mineral compositions of Quaternary sediment samples estimated from XRD analysis results

No.	Lithology	Quartz (%)	Feldspar	Mica	Calcite	Kaolinite	Chlorite	Amphibole
RR01	Silty sand	25	25	15	10	15	10	–
RR02	Silty clay	20	17	20	8	20	15	–
RR03	Fine sand	30	35	15	10	–	5	5
RR04	Fine sand	35	45	10	5	–	5	–
RR05	Medium sand	43	40	6	9	–	2	–

Table 4 Concentrations of total fluoride (Total-F), water soluble fluoride (Ws-F), exchangeable fluoride (Ex-F), fluoride bound to Fe/Mn oxides (Fe/Mn–F), fluoride bound to organic matter (Or-F) and residual fluoride (Residual-F) in two Quaternary sediment samples (in ppm)

No.	Lithology	Total-F	Ws-F	Ex-F	Fe/Mn–F	Or-F	Residual-F
RR01	Silty sand	685.6	46.1	14.5	3.6	7.0	614.4
RR02	Silty clay	757.2	21.7	31.8	27.6	23.0	653.1

aquifers have a larger variation range of TDS values from 375.5 to 1671.3 mg/L, and their pH values change from 7.16 to 7.94.

All four groundwater samples collected from hard rock aquifers have HCO_3^- and Na^+ as the major anion and cation, respectively. Correspondingly, their hydrogeochemical types include HCO_3–Na, $HCO_3{\cdot}SO_4$–Na, and $HCO_3{\cdot}SO_4$–Ca·Na. In the mineral stability diagram of the Na^+–H^+–SiO_2 system (Fig. 2), these four samples all fall within the kaolinite stability field, indicating that the hydrolysis of some alumino-silicate minerals, such as albite and biotite, is responsible for the formation of HCO_3^- and Na^+ that are dominant in the groundwaters. The dissolution of above minerals can produce kaolinite plus cations such as Na^+, Mg^{2+}, and K^+, and the chemical reaction equations are as follows:

$$2NaAlSi_3O_8 + 2CO_2 + 11H_2O = Al_2Si_2O_5(OH)_4 + 2Na^+ + 4H_4SiO_4 + 2HCO_3^- \quad (1)$$

$$2KMg_3AlSi_3O_{10}(OH)_2 + 14CO_2 + 15H_2O = Al_2Si_2O_5(OH)_4 + 2K^+ + 6Mg^{2+} + 4H_4SiO_4 + 14HCO_3^- \quad (2)$$

Moreover, it can be noticed that there are SO_4^{2-} and Ca^{2+} with comparatively higher concentrations in the sample ZX01 and ZX02 (especially in ZX01 whose hydrochemical type is $HCO_3{\cdot}SO_4$–Ca·Na). The existence of gypsum interlayers in aquifer matrix as well as their dissolution should be the mechanism elevating the SO_4^{2-} and Ca^{2+} concentrations in the groundwaters. The dissolution of gypsum can be expressed as the following reaction equation:

$$CaSO_4 \cdot 2H_2O = Ca^{2+} + SO_4^{2-} + 2H_2O \quad (3)$$

Different from the water samples from hard rock aquifers, the hydrochemical type of the three samples of karst groundwaters is HCO_3–Ca·Mg, no matter they are cold or warm (with temperatures higher than 25°C). In other words, HCO_3^- is the dominant anion, and Ca^{2+} and Mg^{2+} are the major cations in these samples. Moreover, SO_4^{2-} was also detected in karst water samples, although its milligram equivalent percents (meq percents) in all three samples are much less than HCO_3^-. Therefore, dissolution of carbonate minerals and gypsum, the major mineral phases in the aquifer matrix, should be the main chemical processes controlling the chemistry of karst groundwaters.

To more accurately evaluate the effect of the dissolution of above minerals on karst water geochemistry, two "types" of calcium, namely "non-gypsum source calcium" and "non-carbonate source calcium", were differentiated from each other and calculated. Assuming all the SO_4^{2-} in the karst groundwaters is from gypsum dissolution, non-gypsum source calcium can be calculated by subtracting the amount of Ca^{2+} equivalent to the amount of SO_4^{2-} from the total Ca^{2+} concentration and expressed as $[Ca^{2+}] - [SO_4^{2-}]$ (in mmol/L). Thus, a plot of non-gypsum source Ca^{2+} against HCO_3^- (Fig. 3) was made, and in this plot, three karst water samples are located closely around the 1:4 relationship line suggesting congruent dissolution of dolomite. Therefore, it should be the dissolution of dolomite rather than calcite that makes the major contribution to the HCO_3^- and Ca^{2+} in the karst groundwaters. Similarly, in the Mg^{2+} against HCO_3^- plot (Fig. 4), three water samples cluster closely with the 1:4 relationship line suggesting congruent dissolution of dolomite, which proves again that dolomite dissolution should be the dominant karstification process in the study area. According to the above analysis, non-carbonate source calcium can be expressed as $[Ca^{2+}] - 0.25\ [HCO_3^-]$ (in mmol/L),

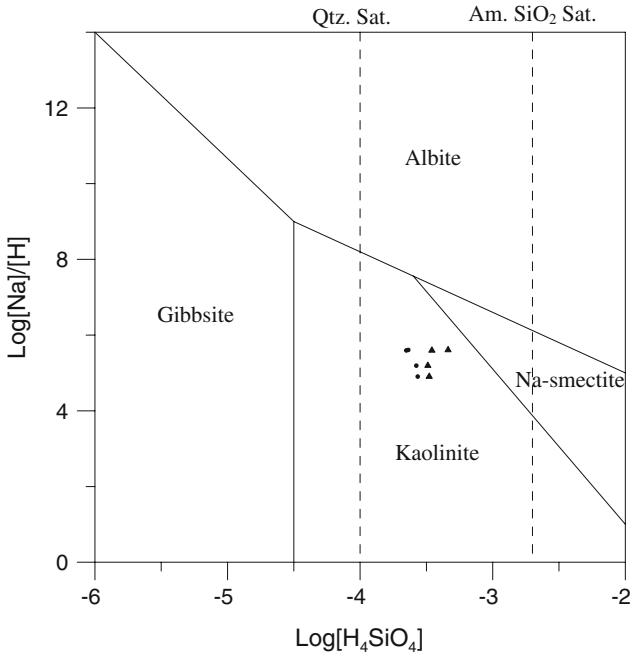

Fig. 2 Selected groundwater samples plotted onto the Na^+–H^+–SiO_2 system equilibrium phase diagram. *Qtz. Sat.* refers to quartz saturation line, and *Am. SiO_2 Sat.* amorphous SiO_2 saturation line. Samples from fissured aquifers (*filled triangle*), samples from Quaternary aquifers (*filled circle*)

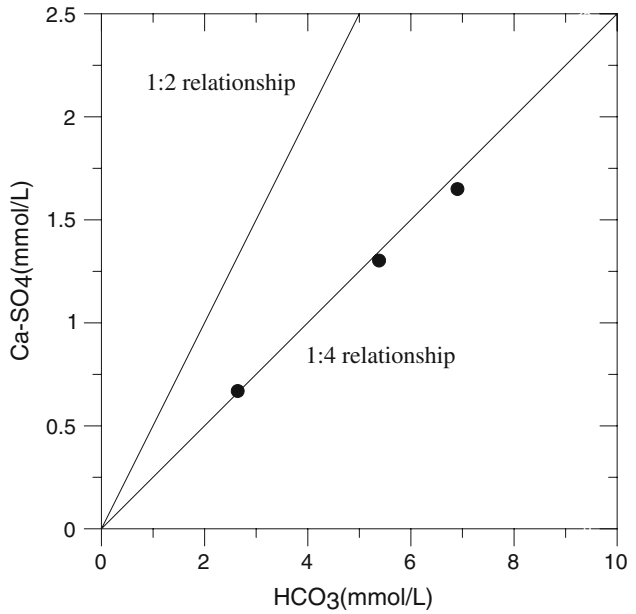

Fig. 3 Plot of non-gypsum source calcium versus bicarbonate. The 1:4 relationship line suggests congruent dissolution of dolomite and the 1:2 relationship line congruent dissolution of calcite. All karst water samples cluster closely with the 1:4 relationship line, indicating the contribution of dolomite dissolution to the calcium and bicarbonate concentrations in the karst groundwaters

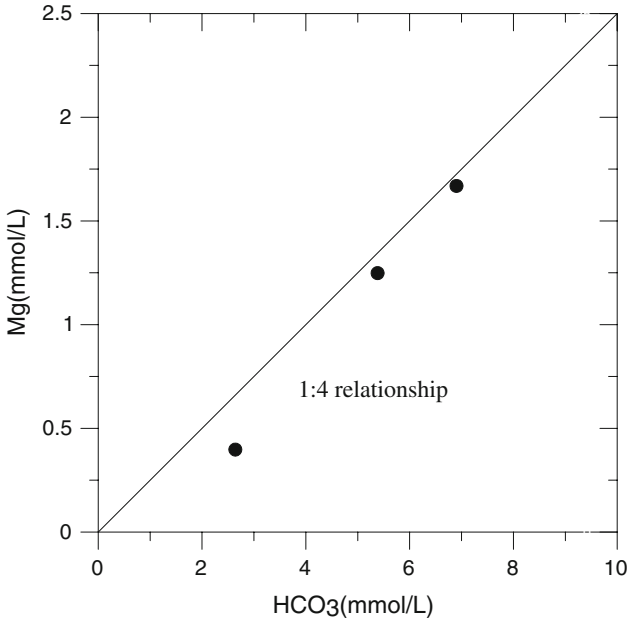

Fig. 4 Plot of magnesium versus bicarbonate. The karst water samples scatter closely around the 1:4 relationship line suggesting congruent dissolution of dolomite

and the multiplier "0.25" was defined according to the stoichiometry of the following reaction:

$$CaMg(CO_3)_2 + 2CO_2 + 2H_2O = Ca^{2+} + Mg^{2+} + 4HCO_3^- \quad (4)$$

The contribution of gypsum dissolution to water chemistry can be seen from a 1:1 linear molarity relationship between non-carbonate Ca^{2+} and SO_4^{2-}. As indicated in Fig. 5, all three water samples are scattered around the 1:1 non-carbonate source Ca^{2+} and SO_4^{2-} relationship line, suggesting congruent dissolution of gypsum.

Similar to the water samples from hard rock aquifers, Quaternary groundwater samples also fall within the kaolinite stability field of the Na^+–H^+–SiO_2 system (Fig. 2), which means that the hydrolysis of primary silicate minerals is yet one of the factors affecting their hydrochemistry. However, compared to the fissure groundwaters and the karst groundwaters, the groundwaters in Quaternary aquifers have more variable hydrochemistry. The chemical types include HCO_3–Ca, HCO_3–Ca·Mg, HCO_3–Na·Ca·Mg, HCO_3·SO_4–Ca·Mg, SO_4·HCO_3–Ca·Mg, and SO_4–Na·Ca. Therefore, other hydrogeochemical processes may be responsible for the formation of certain chemical constituents in some Quaternary groundwater samples as well. According to the mineral analysis results in Table 3, quartz, feldspar and micas are the major minerals of Quaternary sediments, and carbonate minerals, namely calcite, were also identified. Thus, in addition to hydrolysis of silicate minerals, the chemistry of Quaternary groundwaters was

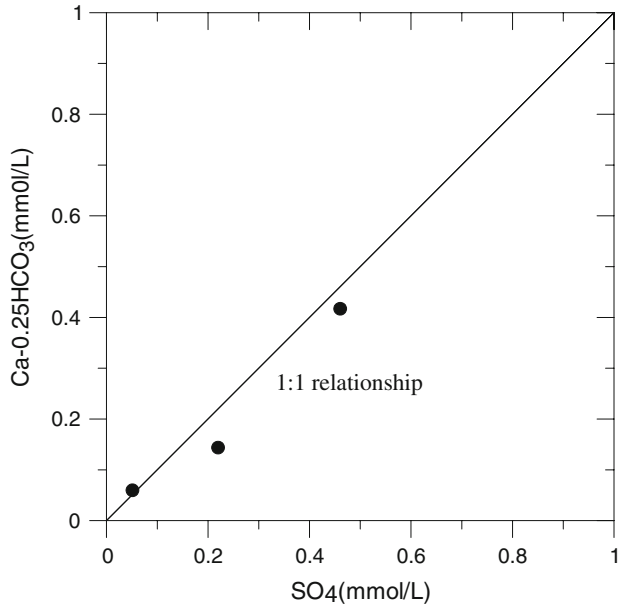

Fig. 5 Plot of non-carbonate source calcium versus sulfate. The karst water samples scatter closely around the theoretical relationship of 1:1 for congruent dissolution of gypsum

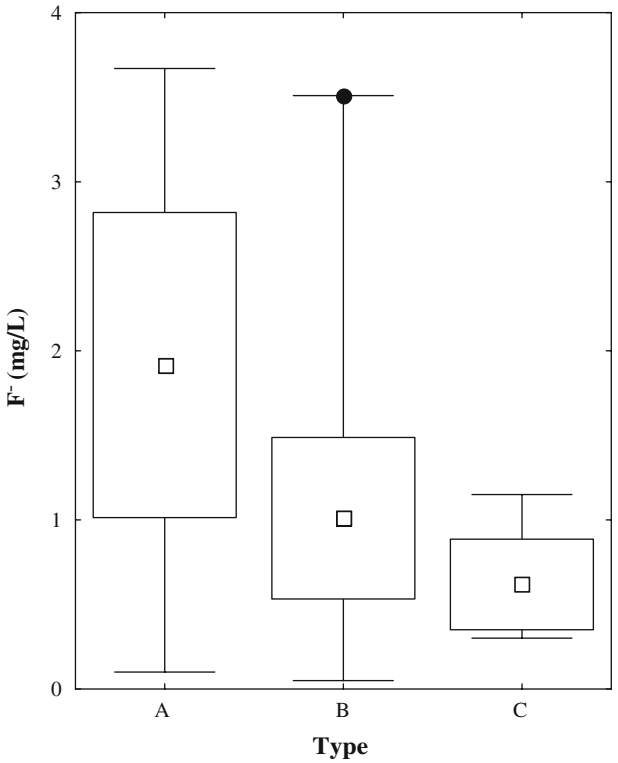

Fig. 6 Box and whisker plot of the fluoride concentrations in water samples of type *A*, *B*, and *C*. Type *A*: water samples from the fissured aquifers, type *B*: water samples from the porous aquifers, type *C*: water samples from the karst aquifers. The *boxes* show the mean value minus standard error, the mean value, and the mean value plus standard error. The smallest and largest values are indicated by the *small horizontal bars* at the end of the whiskers. *Fillesd circle* represents outlier value

also influenced by their reactions with carbonate minerals. Moreover, it is well known that gypsum is widely distributed in Quaternary sediments, although its mass percentage may be so low that it cannot be detected by X-ray powder diffractometry (XRD). Therefore, dissolution of gypsum can increase sulfate concentration in groundwater of Quaternary aquifers. The nitrate concentrations of sample ZX05 (158.0 mg/L), ZX09 (99.3 mg/L), and ZX11 (109.0 mg/L) are very high, indicating that agricultural pollution may have affected the hydrochemistry of Quaternary groundwaters in certain areas.

Source of fluoride in groundwater

The fluoride concentrations of three types of groundwater in the study area were compared in a Box and whisker plot (Fig. 6). It can be clearly seen from Fig. 6 that the average fluoride concentration increases in the following sequence: the karst groundwater, the groundwater in Quaternary aquifers, and the groundwater in hard rock aquifers. Furthermore, the water samples containing fluoride more than 1.5 mg/L were all collected from the hard rock aquifers and the Quaternary aquifers. In other words, there are no high fluoride groundwaters occurring in the karst aquifers. The reason is that the fluoride concentration in groundwater is evidently constrained by solubility control of fluorite, and the comparatively higher concentration of Ca^{2+} in the karst groundwaters prevents fluoride enrichment. In contrast, for the Quaternary groundwaters and the fissure groundwaters, Na^{+} is the dominant cation in many cases because the dissolution of sodium-rich silicate minerals instead of carbonate minerals is usually the major hydrogeochemical process in the aquifers. As Fig. 7 illustrates, the Na/Ca ratios of the water samples from the Quaternary and hard rock aquifers are generally more than those from the karst aquifers, and all four groundwater samples with fluoride concentration more than 1.5 mg/L have very high Na/Ca ratios, which clearly indicates the control of Ca^{2+} on fluoride enrichment in groundwater.

It is interesting to note that the average fluoride concentration of the warm groundwater samples with temperatures more than 25°C is much higher than that of the cold groundwater samples (Fig. 8). This is because high water temperature accelerates the water–mineral interactions in the aquifers, including the dissolution of some fluoride-bearing minerals, such as fluorite.

Genesis of high fluoride groundwater in hard rock aquifers

In four water samples from the hard rock aquifers, two (ZX03 and ZX04) have very high fluoride concentrations

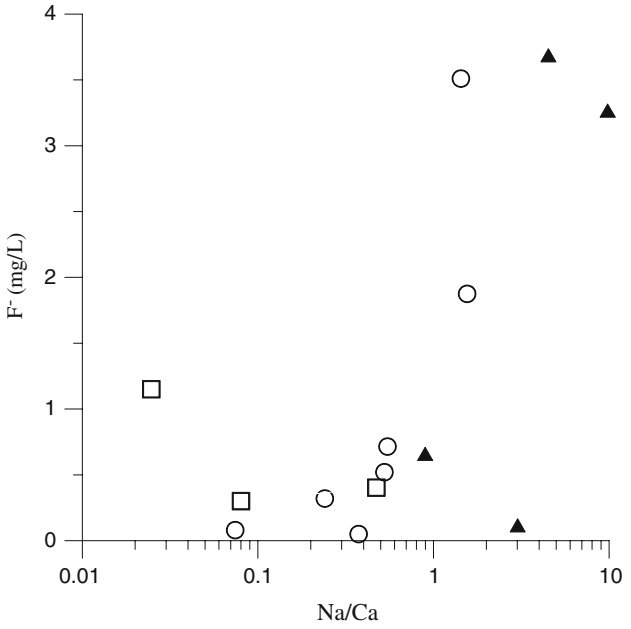

Fig. 7 Fluoride concentration versus [Na]/[Ca] ratio of groundwater samples. Legend of the sample symbols: water samples from the fissured aquifers (*filled rtiangle*), water samples from the porous aquifers (*open circle*), water samples from the karst aquifers (*open square*)

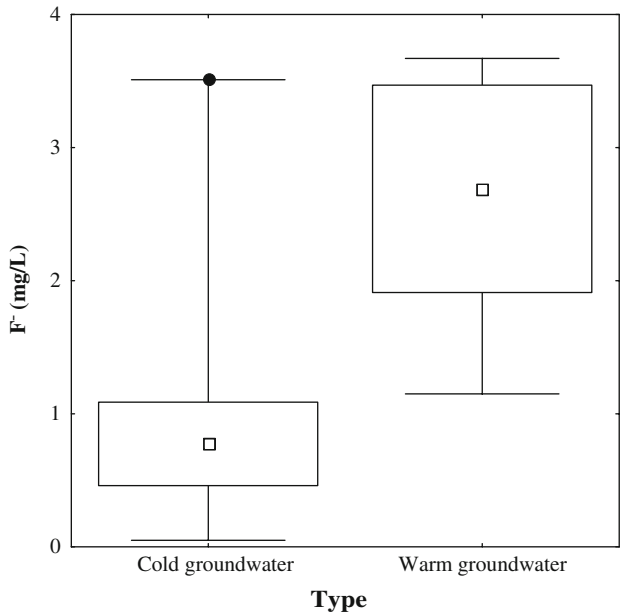

Fig. 8 Box and whisker plot of the fluoride concentrations in warm groundwater samples and cold groundwater samples. The legend is the same as in Fig. 6

more than 1.5 mg/L (3.25 and 3.67 mg/L, respectively), whereas the other two have much lower fluoride concentrations (Table 2). A further inspection indicates that the high fluoride groundwater samples (ZX03 and ZX04) typically have higher pH values (8.03 and 7.96) as

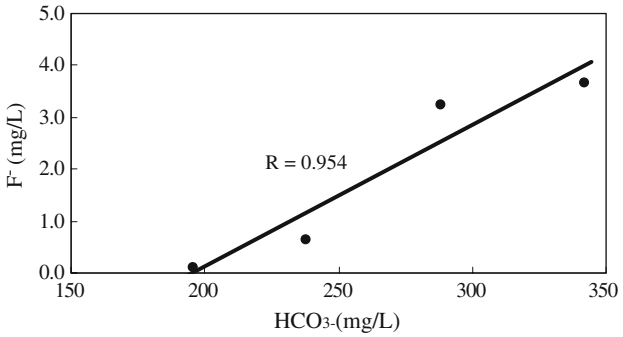

Fig. 9 F^- versus HCO_3^- of groundwater samples from the fissured aquifers. The *trend line* shows the linear relationships with correlation coefficient *R* of 0.954

compared with samples (ZX01 and ZX02) containing less fluoride (the pH values of them being 7.62 and 7.24, respectively). This implies that the high pH may favor the enrichment of fluoride in groundwater. As a matter of fact, plentiful OH^- radicals in groundwater with high pH value can replace the exchangeable F^- of some fluoride-bearing minerals (such as biotite), increasing the F^- concentration in groundwater. For instance:

$$KMg_3[AlSi_3O_{10}]F_2 + 2OH^- = KMg_3[AlSi_3O_{10}][OH]_2 + 2F^- \quad (5)$$

Moreover, it should be noticed that for the water samples from hard rock aquifers, the fluoride concentrations are positively correlated with the HCO_3^- contents, with a very high regression coefficient of 0.954 (Fig. 9). In the granite or sandstone aquifers, fluorite dissolution may be another natural source for fluoride in groundwater. As mentioned above, the hydrolysis of alumino-silicate minerals in the hard rock aquifers generates an amount of HCO_3^-, which can accelerate the dissolution of fluorite by the following reaction:

$$CaF_2 + 2HCO_3^- = CaCO_3 + 2F^- + H_2O + CO_2 \quad (6)$$

Genesis of high fluoride groundwater in Quaternary aquifers

The fluoride concentrations of two Quaternary groundwater samples (ZX09 and ZX10) are more than 1.5 mg/L, whereas those of the other five samples are much less than 1.5 mg/L. To delineate the genesis of high fluoride groundwaters from Quaternary aquifers, the total fluoride concentrations of two aquifer sediment samples collected from the area where the high fluoride groundwaters occur (namely Huangpo village, see Fig. 1) were measured, so were the concentrations of water soluble fluoride (Ws-F), exchangeable fluoride (Ex-F), fluoride bound to Fe/Mn oxides (Fe/Mn–F), fluoride bound to organic matter (Or-F) and residual fluoride (Residual-F) in these two samples.

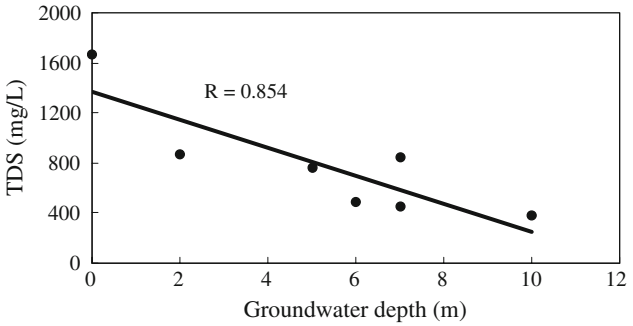

Fig. 10 TDS value versus groundwater depth of samples from the Quaternary aquifers. The *trend line* shows the linear relationships with correlation coefficient *R* of 0.854

The measurement results show that although the Fe/Mn–F and Or-F concentrations of RR01 and RR02 are quite different, both of them have very high concentrations of water soluble fluoride (Ws-F) and exchangeable fluoride (Ex-F). So the abundance of Ws-F and Ex-F in aquifer sediments is one of the most important factors controlling the occurrence of high fluoride groundwaters in Quaternary aquifers.

Furthermore, the high fluoride groundwater samples ZX09 and ZX10 have much higher TDS values than the other groundwater samples from Quaternary aquifers, and in the locations where ZX09 and ZX10 were sampled (Huangpo village), their burial depths are evidently smaller as well (Table 1). The plot of TDS value versus groundwater depth (Fig. 10) also indicates that there is significant negative correlation between them (the regression coefficient being 0.854). The average annual rainfall in recent four decades at Huangpo village is 679.7 mm, much less than the corresponding value of the whole Zhongxiang City. Therefore, the Huangpo village is a comparatively arid area with groundwater burial depth less than or equal to 2 m, and evaporation is responsible for the elevated TDS values in the groundwaters. And as a result of evaporation, Ca^{2+} would precipitate out as $CaCO_3$, reducing Ca^{2+} concentration of the groundwaters. Consequently, the solubility control of CaF_2 on fluoride enrichment in the aqueous phase becomes weaker, and fluoride concentration is elevated in the groundwaters. Furthermore, it is worth noting that the Sr^{2+}/Ca^{2+} ratio (0.014) of sample ZX10 collected at Huangpo is much higher than that of other Quaternary groundwater samples, which also indicates the evaporation and subsequent $CaCO_3$ precipitation occurring at Huangpo. During the evaporation, the concentration of Sr^{2+} in groundwater resulting from the dissolution of strontianite and celestite was hardly affected, and therefore the precipitation of Ca^{2+} can induce the increase of Sr^{2+}/Ca^{2+} ratio.

Conclusions

For the three types of groundwaters occurring in Zhongxiang City, hydrogeochemical processes are different. Dissolution of dolomite and gypsum is the major geochemical process responsible for genesis of hydrochemistry of karst groundwaters, whereas hydrolysis of silicate minerals the prevalent process occurring in the hard rock aquifers. In the Quaternary aquifers, the interactions between groundwaters and several kinds of minerals, such as silicate minerals, carbonate minerals, gypsum, and halite, may affect water chemistry.

The fluoride concentration as high as 3.67 mg/L was detected in the groundwater samples collected in this study. High fluoride groundwater samples with concentrations more than 1.5 mg/L were all from hard rock aquifers and Quaternary aquifers, whereas all water samples from the karst aquifers have fluoride concentrations much less than 1.5 mg/L. It can be concluded that the comparatively higher Ca^{2+} concentrations in the karst groundwaters are unfavorable for fluoride enrichment, due to solubility control of fluorite on fluoride concentration in groundwater. Moreover, the warm groundwaters with temperature more than 25°C generally have higher fluoride concentrations compared to the cold groundwaters, as a result of the intensified reactions of groundwaters with fluoride bearing minerals under higher temperature condition. For the water samples from hard rock aquifers, there exist positive correlations between F^- concentration and HCO_3^- concentration as well as pH value, indicating that the high HCO_3^- concentration can accelerate the dissolution of fluorite to enhance fluoride concentration in groundwater, and the high pH value is helpful for the anion exchange between OH^- in groundwater and exchangeable F^- of some silicate minerals whose hydroxyl group is replaced by F^-. For the Quaternary aquifers, the sediments have very high concentrations of total fluoride, water-soluble fluoride and exchangeable fluoride in the area where the high fluoride groundwaters occur, and therefore the abundance of fluoride in aquifer sediments is one of the favorable conditions for the formation of high fluoride groundwaters. Furthermore, in the high fluoride Quaternary groundwater area, evaporation takes place due to relatively arid climate and very small groundwater burial depth, which evidently increases the HCO_3^- and Ca^{2+} concentrations of the groundwaters, and induces the precipitation of calcite. The decrease of Ca^{2+} concentration caused by calcite precipitation weakens fluorite solubility control and results in fluoride enrichment in groundwater.

Acknowledgments This work was financially supported by Open Fund of State Key Laboratory of Environmental Geochemistry, Natural Science Foundation of Hubei Province of China (No.

2007ABA312), National Natural Science Foundation of China (No. 40702041 and 40425001), China Postdoctoral Science Foundation (No. 200801333), Open Fund of State Key Laboratory of Geological Processes and Mineral Resources (No. GPMR200714), and Open Fund of MOE Key Laboratory of Biogeology and Environmental Geology (No. BGEGF200813). The manuscript benefited a lot from the constructive comments of an anonymous reviewer.

References

Apambire WB, Boyle DR, Michel FA (1997) Geochemistry, genesis, and health implications of fluoriferous groundwaters in the upper regions of Ghana. Env Geol 33(1):13–24. doi:10.1007/s002540050221

Appelo CAJ, Postma D (1996) Geochemistry, groundwater, and pollution. Balkema, Rotterdam

Cao S (1990) Scientific works on prevention and remediation for endemic fluorosis. In: Zhang Y (ed) Four decades of prevention and remediation for endemic diseases in China (in Chinese). China Environmental Science Press, Beijing

Cao J, Zhao Y, Liu J (1997) Brick tea consumption as the cause of dental fluorosis among children from Mongol, Kazak and Yugu populations in China. Food Chem Toxicol 35:827–833. doi:10.1016/S0278-6915(97)00049-5

Cao J, Zhao Y, Liu J (2000) Fluoride in the environment and brick-tea-type fluorosis in Tibet. J Fluor Chem 106:93–97. doi:10.1016/S0022-1139(00)00310-9

Dai S, Ren D, Ma S (2004) The cause of endemic fluorosis in western Guizhou Province, Southwest China. Fuel 83:2095–2098. doi:10.1016/j.fuel.2004.03.016

Datta PS, Deb DL, Tyagi SK (1996) Stable isotope (^{18}O) investigations on the processes controlling fluoride contamination of groundwater. J Contam Hydrol 24:85–96. doi:10.1016/0169-7722(96)00004-6

Gaciri SJ, Davies TC (1993) The occurrence and geochemistry of fluoride in some natural waters of Kenya. J Hydrol 143:395–412. doi:10.1016/0022-1694(93)90201-J

Gizaw B (1996) The origin of high bicarbonate and fluoride concentrations in waters of the main Ethiopian Rift Valley. J Afr Earth Sc 22:391–402. doi:10.1016/0899-5362(96)00029-2

Grimaldo M, Borja-Aburto VH, Ramirez AL, Ponce M, Rosas M, Diaz-Barrjga F (1995) Endemic fluorosis in San Luis Potosi, Mexico. 1. Identification of risk factors associated with human exposure to fluoride. Environ Res 68:25–30. doi:10.1006/enrs.1995.1004

Gupta MK, Singh V, Rajwanshi P, Agarwal M, Rai K, Srivastava S, Shrivastav R, Dass S (1999) Groundwater quality assessment of tehsil kheragarh, agra (India) with special reference to fluoride. Environ Monit Assess 59:275–285. doi:10.1023/A:1006117604763

Jacks G, Bhattacharya P, Chaudhary V, Singh KP (2005) Controls on the genesis of some high-fluoride groundwater in India. Appl Geochem 20:221–228. doi:10.1016/j.apgeochem.2004.07.002

Karro E, Indermitte E, Saava A, Haamer K, Marandi A (2006) Fluoride occurrence in publicly supplied drinking water in Estonia. Env Geol 50:389–396. doi:10.1007/s00254-006-0217-1

Krishnamachari KA (1986) Skeletal fluorosis in humans: a review of recent progress in the understanding of the disease. Prog Food Nutr Sci 10:279–314

Liang CK (1993) Study on dose-effect relationship in coal combustion fluorosis endemic area population (in Chinese with English Abstract). J Hyg Res 22(3):1–10

Luo H, Yang Z (2000) The environmental geographical analyses of the epidemic fluorosis in Hubei province. J Beijing Norm Univ (Nat Sci) 36:122–126 (in Chinese with English Abstract)

Moturi WK, Tole MP, Davies TC (2002) The contribution of drinking water towards dental fluorosis: A case study of Njoro Division, Nakuru District, Kenya. Environ Geochem Health 24:123–130. doi:10.1023/A:1014204700612

Nanyaro JT, Aswathanarayana U, Mungere JS, Lahermo P (1984) A geochemical model for the abnormal fluoride concentrations in waters in parts of northern Tanzania. J Afr Earth Sci 2:129–140

Rao NS, Devadas DJ (2003) Fluoride incidence in groundwater in an area of Peninsular India. Env Geol 45:243–251. doi:10.1007/s00254-003-0873-3

Rukah YA, Alsokhny K (2004) Geochemical assessment of groundwater contamination with special emphasis on fluoride concentration, North Jordan. Chemie der Erde-Geochemistry 64:171–181. doi:10.1016/j.chemer.2003.11.003

Rwenyonyi CM, Birkeland JM, Haugejorden O, Bjorvatn K (2000) Age as a determinant of severity of dental fluorosis in children residing in areas with 0.5 and 2.5 mg fluoride per liter in drinking water. Clin Oral Investig 4:157–161. doi:10.1007/PL00010677

Saxena VK, Ahmed S (2003) Inferring the chemical parameters for the dissolution of fluoride in groundwater. Env Geol 43:731–736

Vieira APGF, Hanocock R, Eggertsson H, Everett ET, Grynpas MD (2005) Tooth quality in dental fluorosis: genetic and environmental factors. Calcif Tissue Int 76:17–25. doi:10.1007/s00223-004-0075-3

Wang L, Huang J (1995) Outline of control practice of endemic fluorosis in China. Soc Sci Med 41(8):1191–1195. doi:10.1016/0277-9536(94)00429-W

WHO (World Health Organization (1984) Guidelines for drinking water quality. Drinking water quality control in small community supplies, vol 3. WHO, Geneva

Wu L, Tang S, Gong X, Huang W (1999) Evaluation and analysis of effect for defluoridation of endemic fluorosis of Hubei province (in Chinese with English Abstract). Chinese J Endemiol 18:279–280